

Electrical Properties of New Organic Conductor (BEST)₂InBr₄ [BEST = Bis(ethylenediseleno)tetrathiafulvalene] up to 10.8 GPa and Antiferromagnetic Transition of (BEST)₂FeBr₄

Hengbo Cui,[†] James Brooks,^{*,†} David Graf,[†] Yoshinori Okano,[‡] Haoling Sun,^{‡,§} and Hayao Kobayashi[⊥]

National High Magnetic Field Laboratory (NHMFL), Florida State University, Tallahassee, Florida 32310, Institute for Molecular Science, Okazaki 444-8585, Japan, and Department of Chemistry, College of Humanities and Science, Nihon University, Sakurajosui, Setagaya-ku, Tokyo 156-8550, Japan

Received February 3, 2009

A new organic conductor, (BEST)₂InBr₄, with alternating donor layer arrangement has been synthesized, and the electrical properties have been investigated up to 10.8 GPa. The temperature dependence of the high-pressure resistivity shows a complicated metal–semiconductor transition behavior. The room temperature resistivity decreases with pressure up to 8.6 GPa but increases at higher pressures. The magnetic susceptibility of an isostructural (BEST)₂FeBr₄ salt shows an antiferromagnetic transition at 4.4 K, which is suppressed with increasing magnetic field.

Since the development of magnetic organic conductors such as the antiferromagnetic superconductor κ -(BETS)₂-FeBr₄ [BETS = bis(ethylenedithio)tetraselenafulvalene],¹ the ferromagnetic metal (ET)₃[MnCr(C₂O₄)₃](CH₂Cl₂) [ET = (ethylenedithio)tetrathiafulvalene],² and the magnetic field-induced superconductor λ -(BETS)₂FeCl₄,³ numerous efforts have been made to combine conducting and magnetic properties. However, so far only five materials based on two donor systems have reached the goal of coexisting metallic

and antiferromagnetic ordered states.^{1,4,5} In this work, we consider the π -electron interaction with localized 3d moments caused by close contact between chalcogen atoms and magnetic anions. We selected an isomer of the BETS donor, BEST [bis(ethylenediseleno)tetrathiafulvalene], in which Se atoms protrude in the six-membered rings to construct a new magnetic organic configuration. The Se atoms have larger electron cloud diameters than S, which can lead to an enhancement of the π -d interactions. However, all previous such work has led to semiconducting or insulating behavior at low temperatures (<150 K) and ambient pressure.^{6,7} However, in one case, κ -(BEST)₂Cu[N(CN)₂]Br exhibited a metal-to-insulator transition at 25 K and, at a pressure of 1.5 kbar, showed a superconducting transition at 7.5 K.⁶ High pressure is useful to increase weak transverse transfer integrals and can often stabilize a low-temperature metallic state. In addition, pressure can reveal new properties, as is the case of the highest superconducting transition temperature ($T_c = 14.2$ K at 8.2 GPa) in an organic conductor found in

* To whom correspondence should be addressed. E-mail: brooks@magnet.fsu.edu.

[†] Florida State University.

[‡] Institute for Molecular Science.

[§] Present address: Department of Chemistry, Beijing Normal University, Beijing 100875, People's Republic of China.

[⊥] Nihon University.

- (1) (a) Ojima, E.; Fujiwara, H.; Kato, K.; Kobayashi, H.; Tanaka, H.; Kobayashi, A.; Tokumoto, M.; Cassoux, P. *J. Am. Chem. Soc.* **1999**, *121*, 5581–5582. (b) Fujiwara, H.; Ojima, E.; Nakazawa, Y.; Narymbetov, B. Zh.; Kato, K.; Kobayashi, H.; Kobayashi, A.; Tokumoto, M.; Cassoux, P. *J. Am. Chem. Soc.* **2001**, *123*, 306–314.
- (2) Coronado, E.; Galán-Mascarós, J. R.; Gómez-García, C. J.; Laukhin, V. *Nature (London)* **2000**, *408*, 447–449.
- (3) (a) Uji, S.; Shinagawa, H.; Terashima, T.; Yakabe, T.; Terai, Y.; Tokumoto, M.; Kobayashi, A.; Tanaka, H.; Kobayashi, H. *Nature (London)* **2001**, *410*, 908–910. (b) Fujiwara, H.; Kobayashi, H.; Fujiwara, E.; Kobayashi, A. *J. Am. Chem. Soc.* **2002**, *124*, 6816–6817.
- (4) Otsuka, T.; Kobayashi, A.; Miyamoto, Y.; Kikuchi, J.; Wada, N.; Ojima, E.; Fujiwara, H.; Kobayashi, H. *Chem. Lett.* **2000**, 732, 733.

- (5) (a) Fujiwara, H.; Wada, K.; Hiraoka, T.; Hayashi, T.; Sugimoto, T.; Nakazumi, H.; Yokogawa, K.; Teramura, M.; Yasuzuka, S.; Murata, K.; Mori, T. *J. Am. Chem. Soc.* **2005**, *127*, 14166–14167. (b) Hayashi, T.; Xiao, X.; Fujiwara, H.; Sugimoto, T.; Nakazumi, H.; Noguchi, S.; Fujimoto, T.; Yasuzuka, S.; Yoshino, H.; Murata, K.; Mori, T.; Aruga-Katori, H. *J. Am. Chem. Soc.* **2006**, *128*, 11746–11747. (c) Xiao, X.; Hayashi, T.; Fujiwara, H.; Sugimoto, T.; Noguchi, S.; Weng, Y.; Yoshino, H.; Murata, K.; Aruga-Katori, H. *J. Am. Chem. Soc.* **2007**, *129*, 12618–12619.
- (6) Sakata, J.; Sato, H.; Miyazaki, A.; Enoki, T.; Okano, Y.; Kato, R. *Solid State Commun.* **1998**, *108*, 377–381.
- (7) (a) Wang, H. H.; Montgomery, L. K.; Geiser, U.; Porter, L. C.; Carlson, K. D.; Ferraro, J. R.; Williams, J. M.; Cariss, C. S.; Rubinstein, R. L.; Whitworth, J. R.; Evain, M.; Novoa, J.; Whangbo, M.-H. *Chem. Mater.* **1989**, *1*, 140–148. (b) Lyubovskiyar, R. N.; Zhilyaeva, E. I.; Torunova, S. A.; Bogdanova, O. A.; Konovalikhin, S. V.; Dyachenko, O. A.; Lyubovskii, R. B. *Synth. Met.* **1997**, *85*, 1581–1582. (c) Clemente-León, M.; Coronado, E.; Galán-Mascarós, J. R.; Gimenez-Saiz, C.; Gómez-García, C. J.; Fabre, J. M.; Mousdis, G. A.; Papavassiliou, G. C. *J. Solid State Chem.* **2002**, *168*, 616–625. (d) Cui, H.; Otsubo, S.; Okano, Y.; Kobayashi, H. *Chem. Lett.* **2005**, *134*, 254–255. (e) Coronado, E.; Curreli, S.; Gimenez-Saiz, C.; Gómez-García, C. J.; Alberola, A. *Inorg. Chem.* **2006**, *45*, 10815–10824.

β' -(ET)₂ICl₂.⁸ Here we report organic conductors of (BEST)₂MBr₄ (M = Fe, In), which exhibit metallic behavior around room temperature.

Black platelike crystals were grown by electrochemical oxidation from a solution of 90% chlorobenzene and 10% ethanol containing BEST (4 mg) and tetrabutylammonium salts of FeBr₄⁻ and InBr₄⁻ (40 mg). A constant current of 0.1 μ A was applied for 2 weeks. The conductivity was measured by a conventional four-probe method from room temperature to 1.5 K. The lower pressure measurements were made for both FeBr₄ and InBr₄ salts using a Be–Cu clamp cell with Daphne 8686 oil as the pressure medium. Measurements above 2 GPa were also made for InBr₄ salt, where a diamond anvil cell (DAC) was used. Gold wires of 5 μ m were attached to the sample with gold paint and placed in the sample chamber of the DAC with a top surface diameter of 700 μ m. Inconel 625 was used as a metal gasket, a mixture fluorinert (3M) 1:1 of FC-70 and FC-72 was used for the pressure medium, and the pressure was determined from ruby fluorescence at room temperature. The sample mounting method has been previously reported.⁹

Single-crystal structure determinations of (BEST)₂MBr₄ (M = Fe, In) reveal that both crystals have almost the same crystal structure.¹⁰ As shown in Figure 1a, there are two crystallographically independent BEST molecules stacked along the *b* axis that form the columns, arrayed side by side to make two independent donor layers (or conduction layers) arranged alternately along the *c* axis. There are many close S (Se)···Se (S) contacts (\AA) in the conduction layers (e.g., Se···Se = 3.50, 3.529, 3.556, and 3.623 \AA ; Se···S = 3.69, 3.72, 3.73, 3.75, 3.76, and 3.78 \AA) in (BEST)₂FeBr₄. There are also many Se···Br contacts much shorter than the corresponding van der Waals distance (3.95 \AA ; see Figure 1a).

The Fermi surfaces of (BEST)₂FeBr₄ were calculated using an extended Hückel tight-binding band approximation based on the room temperature crystal structures.¹¹ Because the interlayer interaction is very weak, the two independent layers yield two quasi-one-dimensional open Fermi surfaces (see Figure 1c). The Fermi surfaces originate from two crystallographically independent donor layers: the charge distribu-

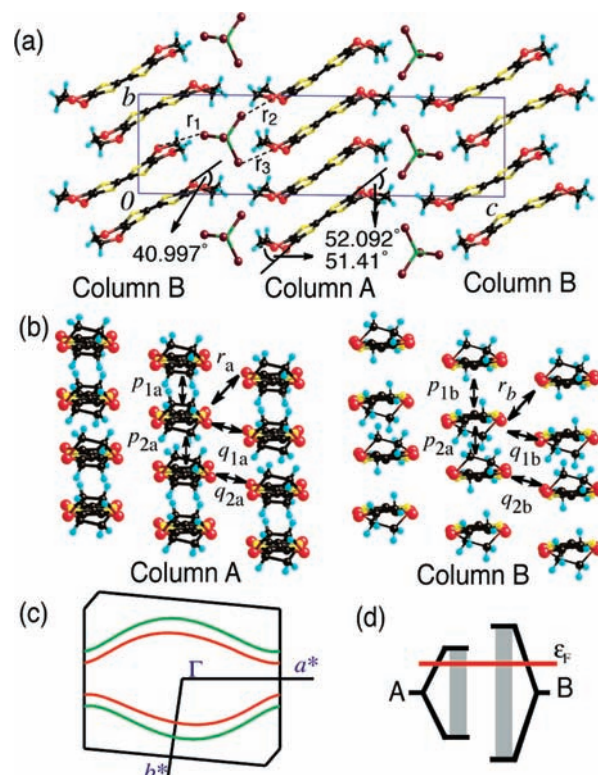


Figure 1. Crystal structure and Fermi surface of (BEST)₂FeBr₄. (a) Structure projected along the *a* axis. The dotted lines (r_1 , r_2 , r_3) indicate the representative short Se···Br contacts: 3.479 \AA (r_1), 3.502 \AA (r_2), 3.69 \AA (r_3). (b) Arrangement of BEST molecules projected along the long axis of the molecule with interdonor transfer integrals. The in-stack overlap integrals are $p_{1a} = 9.3 \times 10^{-3}$, $p_{2a} = 9.8 \times 10^{-3}$ (layer A) and $p_{1b} = 14.3 \times 10^{-3}$, $p_{2b} = 10.4 \times 10^{-3}$ (layer B) and the intrastack overlaps are $r_a = -0.63 \times 10^{-3}$, $q_{1a} = 1.3 \times 10^{-3}$, $q_{2a} = 0.87 \times 10^{-3}$ (layer A) and $r_b = -1.8 \times 10^{-3}$, $q_{1b} = 1.6 \times 10^{-3}$, $q_{2b} = 1.5 \times 10^{-3}$ (layer B). (c) Quasi-one-dimensional open Fermi surface from the two different donor columns. The green and red lines correspond to Fermi surfaces of layers B and A, respectively. (d) Illustration of the band scheme of (BEST)₂FeBr₄ explaining the origin of the existence of two pairs of Fermi surfaces.

tion derived from the band calculation is $A^{0.42}B^{0.58}$,¹² originating from the difference in the bandwidths of layers A and B (see Figure 1d). Because the periodic charge modulation in molecular conductors usually originates from the intermolecular Coulomb interactions, it is interesting that the band structure of (BEST)₂FeBr₄ provides another very simple mechanism for charge modulation. However, further studies are needed to confirm the periodic charge modulation in (BEST)₂FeBr₄.

(BEST)₂FeBr₄ remains metallic^{7c} down to 180 K at ambient pressure [$\sigma(RT) = 25 \text{ S cm}^{-1}$]. High-pressure resistivity measurements showed that at 1.2 GPa the metallic state is stabilized down to about 40 K (Figure 2a). (BEST)₂InBr₄ exhibits a metallic behavior above 250 K at ambient pressure (Figure 2b). The room temperature resistivity decreases up to 8.6 GPa and then increases at higher pressure. The metallic state persists down to 28 K at 5.8 GPa (Figure 2c). Above 5.8 GPa, the metallic state is no longer favored, and at higher pressures, a semiconducting state over a wider range of temperatures emerges (Figure

(12) The charges are calculated by two molecular band fillings at Fermi levels. The bond lengths of the central C=C in A and B molecules are 1.41(6) and 1.34(7) \AA , respectively.

(8) Taniguchi, H.; Miyashita, M.; Uchiyama, K.; Satoh, K.; Mōri, N.; Okamoto, H.; Miyagawa, K.; Kanoda, K.; Hedo, M.; Uwatoko, Y. *J. Phys. Soc. Jpn.* **2003**, *72*, 468–471.

(9) (a) Adachi, T.; Tanaka, H.; Kobayashi, H.; Miyazaki, T. *Rev. Sci. Instrum.* **2001**, *72*, 2358–2360. (b) Cui, H.; Okano, Y.; Zhou, B.; Kobayashi, A.; Kobayashi, H. *J. Am. Chem. Soc.* **2008**, *130*, 3738–3739.

(10) The lattice constants of (BEST)₂MBr₄ (M = Fe, In) are reproduced here:^{7c} space group *P* $\bar{1}$, $a = 6.175(3) \text{ \AA}$, $b = 8.335(4) \text{ \AA}$, $c = 33.32(2) \text{ \AA}$, $\alpha = 89.43(1)^\circ$, $\beta = 89.14(1)^\circ$, $\gamma = 84.63(1)^\circ$, $V = 1856 \text{ \AA}^3$,^{7c} and $R_1 = 0.066$ for M = Fe; space group *P* $\bar{1}$, $a = 6.725(1) \text{ \AA}$, $b = 8.362(1) \text{ \AA}$, $c = 33.554(5) \text{ \AA}$, $\alpha = 90.154(3)^\circ$, $\beta = 90.453(3)^\circ$, $\gamma = 95.206(3)^\circ$, $V = 1879.2 \text{ \AA}^3$, and $R_1 = 0.041$ for M = In. The crystallographic data [CCDC 718566 and 718567] can be obtained free of charge from www.ccdc.cam.ac.uk/data_request/cif.

(11) The exponents and the ionization potentials (eV) for atomic orbitals are as follows: Se 4s, 2.122, –20.0; Se 4p, 1.827, –11.0; S 3s, 2.122, –22.0; S 3p, 1.827, –10.5; C 2s, 1.625, –21.4; C 2p, 1.625, –11.4; H 1s, 1.0, –13.6.

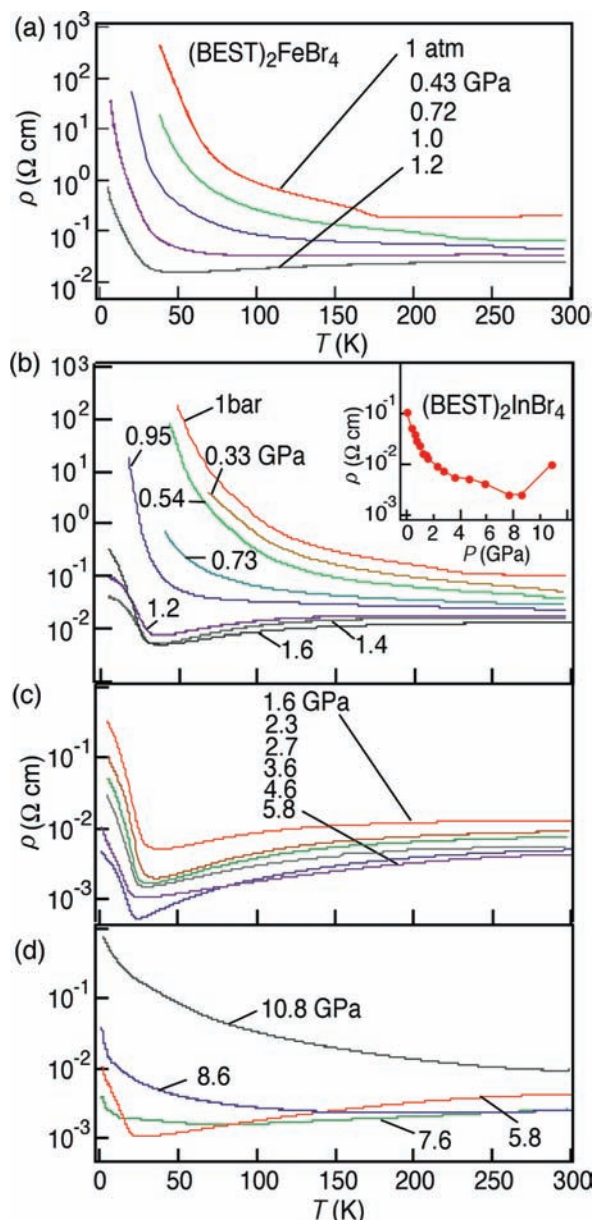


Figure 2. Resistivity: (a) $(\text{BEST})_2\text{FeBr}_4$ (clamp cell). (b) $(\text{BEST})_2\text{InBr}_4$ below 1.6 GPa (clamp cell). The pressure dependence of the room temperature resistivity up to 10.8 GPa is also presented. (c) $(\text{BEST})_2\text{InBr}_4$ between 1.6 and 5.8 GPa (DAC). (d) $(\text{BEST})_2\text{InBr}_4$ between 5.8 and 10.8 GPa (DAC).

2d). Here the resistivity minima for 5.8, 7.6, and 8.6 GPa are observed at 28, 77, and 198 K, respectively. At 10.8 GPa, the resistivity is completely semiconducting, with an activation energy of about 9 meV down to 2.5 K.

The magnetic susceptibilities of polycrystalline samples of $(\text{BEST})_2\text{MBr}_4$ ($M = \text{Fe}, \text{In}$) were measured with a SQUID susceptometer between 2 and 300 K in a magnetic field of 0.5 T. As shown Figure 3, the temperature dependence of the susceptibility of the FeBr_4 salt shows a Curie–Weiss behavior with Weiss temperature $\Theta = -5.4$ K and Curie constant $C = 4.858$ K emu mol $^{-1}$ [the contribution of $\text{Fe}^{3+}(d^5)$ is $C = 4.377$ K emu mol $^{-1}$]. The Fe^{3+} 3d spins are

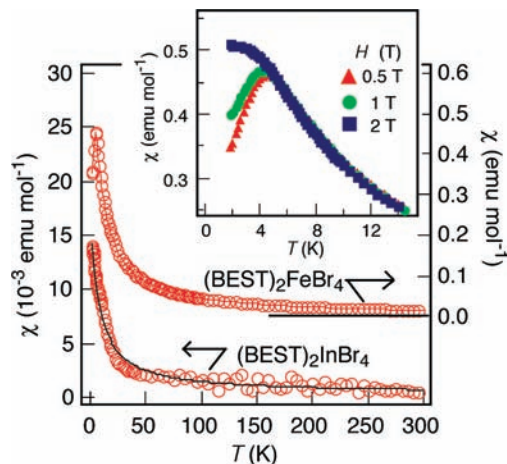


Figure 3. Magnetic properties of $(\text{BEST})_2\text{MBr}_4$ ($M = \text{Fe}, \text{In}$). The inset shows the details of the magnetic field dependence of the antiferromagnetic transition in $(\text{BEST})_2\text{FeBr}_4$.

antiferromagnetically ordered below Neel temperature $T_N = 4.4$ K. As discussed above, there are many short contacts between Br and the BEST molecules, and the Fe 3d spins can interact indirectly through the donor π orbitals. In light of this, $(\text{BEST})_2\text{FeBr}_4$ represents a new organic metal with π –d interactions. The temperature dependence of susceptibility for various magnetic fields is shown in the inset of Figure 3, indicating that the antiferromagnetic order is almost completely suppressed by 2 T. For comparison, the isostructural InBr_4 salt exhibits a conventional Curie–Weiss behavior with a room temperature susceptibility of 5.8×10^{-4} emu mol $^{-1}$, consistent with the paramagnetic contribution of the π -conduction electrons (see Figure 3).

In conclusion, we have performed high-pressure resistivity and magnetic measurements on $(\text{BEST})_2\text{MBr}_4$ ($M = \text{Fe}, \text{In}$). The complicated pressure-induced metal-to-semiconducting transitions observed in the InBr_4 salt are most likely due to the two independent columns that comprise the inequivalent conducting layers. The FeBr_4 salt shows antiferromagnetic ordering with a transition temperature of 4.4 K. The transition temperature is relatively high compared with other antiferromagnetic molecular metals. These results shed new light on the magnetic organic conductors and reveal new aspects of organic conductors at high pressures, especially where lower crystallographic symmetry is present. The electrical and magnetic properties of the FeBr_4 salt under high pressure and magnetic field are still in progress.

Acknowledgment. We thank Dr. S. Tozer for use of the ruby fluorescence system and the NSF (Grant DMR-0602859 to J.B. and Grant DMR-0654118 to NHMFL) for partial support.

Supporting Information Available: X-ray crystallographic files of $(\text{BEST})_2\text{MBr}_4$ ($M = \text{Fe}, \text{In}$) in CIF format. This material is available free of charge via the Internet at <http://pubs.acs.org>.

IC900220G